NJC

ROYAL SOCIETY OF CHEMISTRY

PAPER

View Article Online
View Journal

Cite this: DOI: 10.1039/d5nj01545f

Small extracellular vesicles derived from interstitial cells enhance muscle injury repair and regeneration†

Nana Wang,‡[ab] Xing Pei,‡[c] Yaxuan Feng,[a] Lu Sun,[a] Chao Zhang,[de] Seungjin Lee*[f] and Fei Yu*[a]

Critical limb ischemia (CLI), an advanced stage of peripheral arterial disease, is identified by severe ischemia, rest pain, and tissue necrosis, and possibly leads to amputation if untreated. Cell therapies offer treatment options for CLI by alleviating resting pain and improving the condition of damaged tissues. However, it may mediate immune rejection reactions after cell transplantation and cell activities are susceptible to environmental influences. Small extracellular vesicles (sEV) have emerged as a promising approach for the treatment of CLI, as these carry a lot of the active substances of cells during their formation process. In this study, we investigated the potential of small extracellular vesicles secreted by interstitial cells (IC-sEV) to restore tissue functions and repair ischemic tissue. Our results demonstrated that IC-sEV could effectively promote the proliferation, migration and tube formation of HUVECs. Moreover, IC-sEV had a more pronounced effect on promoting the expression of angiogenic factors in HUVECs compared to ASC-sEV. The therapeutic effect of IC-sEV was further investigated using an *in vivo* animal model of limb ischemia. These data demonstrated that IC-sEV significantly improved blood perfusion in ischemic limbs, promoted the recovery of limb functions, and reduced the extent of ischemic tissue damage. Further analysis revealed that IC-sEV promoted microvascular densities, markedly decreased infiltration, cell apoptosis and fibrosis in the ischemic limbs. In conclusion, IC-sEV transplantation is expected to become a new alternative for the treatment of CLI.

Received 9th April 2025,
Accepted 27th June 2025

DOI: 10.1039/d5nj01545f

rsc.li/njc

1. Introduction

Peripheral artery disease (PAD) represents a prevalent and underappreciated condition characterized by atherosclerotic narrowing or blockage of the arteries supplying the extremities, predominantly the lower limbs.[1,2] Affecting over 200 million people globally, PAD is linked to a notably heightened risk of cardiovascular problems, including morbidity and mortality.[3,4] Critical limb ischemia (CLI), the most severe end of the PAD, is characterized by persistent ischemia that results in ischemic ulcers or gangrene.[5] In the clinical management of CLI, the primary strategy is vascular reconstruction, including endovascular and surgical methods, along with symptom-easing medications.[6,7] Nevertheless, approximately 20–30% of CLI patients may not be candidates for these treatments due to unsuitable arterial targets or other severe comorbidities.[8] In such cases, amputation may be the last option to prolong life, significantly diminishing the patients' quality of life.[9] Given the complexity of the pathological environment in CLI, a more rigorous approach and further research are imperative to explore new avenues of treatment.

Cell therapies have emerged as promising treatment options for CLI, offering a feasible approach to combat ischemia. The mobilization of endogenous cells or the exogenous administration of a large group of cells, such as mesenchymal stem cells (MSCs) and mononuclear cells, can foster structural regeneration and functional repair in damaged tissues.[10,11] This therapeutic

[a] *Tianjin Key Laboratory on Technologies Enabling Development of Clinical Therapeutics and Diagnostics, School of Pharmacy, Tianjin Medical University, Tianjin, 300070, China. E-mail: feiyu@tmu.edu.cn*
[b] *Changzhi Key Laboratory of Drug Molecular Design and Innovative Pharmaceutics, School of Pharmacy, Changzhi Medical College, Shanxi, 046000, China*
[c] *Tianjin Key Laboratory of Food and Biotechnology, School of Biotechnology and Food Science, Tianjin University of Commerce, Tianjin, 300134, China*
[d] *Department of Bone and Soft Tissue Tumor, Key Laboratory of Cancer Prevention and Therapy, Tianjin Medical University Cancer Institute and Hospital, National Clinical Research Center for Cancer, Tianjin's Clinical Research Center for Cancer, Tianjin, 300060, China*
[e] *The Sino-Russian Joint Research Center for Bone Metastasis in Malignant Tumor, Tianjin, China*
[f] *Department of Pharmacy, College of Pharmacy, Ewha Womans University, Seoul, 03760, Republic of Korea. E-mail: sjlee@ewha.ac.kr*

† Electronic supplementary information (ESI) available. See DOI: https://doi.org/10.1039/d5nj01545f

‡ These authors contributed equally to this work.

approach has been extensively validated in animal models, particularly in hindlimb ischemic mouse models, demonstrating its potential for treating CLI.[12–14] Although clinical trials have further confirmed the efficacy of cell therapy in alleviating rest pain and reducing amputation rates, its clinical translation remains limited by inherent tumorigenic risks and persistent technical barriers to achieving sustained engraftment, both of which critically impede broader clinical applications.[15,16] Several research studies have demonstrated that cells exert regenerative potential post-transplantation primarily through various therapeutic effects, including paracrine actions, anti-inflammatory effects and angiogenesis. Notably, the paracrine effect of cells plays a crucial role in their regenerative capacity, primarily due to the secretion of bioactive molecules such as growth factors, cytokines, and extracellular vesicles. Cells mediate therapeutic effects by interacting with surrounding cells and the extracellular matrix through these bioactive molecules.[17,18] Recently, the pivotal role of small extracellular vesicles has gained broad attention in the paracrine actions.[19,20] Therefore, a thorough investigation of the role of small extracellular vesicles in regenerative medicine is essential for the development of novel therapeutic strategies that could revolutionize the treatment of CLI.

Small extracellular vesicles secreted by a multitude of cell types are richly encapsulated with a variety of bioactive molecules inherited from their parent cells, including lipids, nucleic acids, and other significant biological macromolecules.[21] These encapsulated molecules, such as microRNAs (miRNAs), are crucial for intercellular communication and contribute significantly to a spectrum of physiological and pathological processes. Studies have revealed that miRNAs within small extracellular vesicles facilitated unidirectional transfer between cells, inducing phenotypic alterations in recipient cells that can be either transient or enduring. Moreover, miRNAs have been implicated in critical biological processes including angiogenesis, hematopoiesis, and tumorigenesis.[22–24] The biological function of small extracellular vesicles is closely related to the cell type of origin.[25–27] Small extracellular vesicles released by dendritic cells have been shown to possess the remarkable ability to identify and eliminate cancer cells within tumor microenvironments, suggesting a role in immune surveillance and cancer therapy.[28] Similarly, platelet-derived small extracellular vesicles have significantly enhanced cardiac function recovery in a murine model of cardiac ischemia/reperfusion injury, highlighting the therapeutic potential of small extracellular vesicles derived from cells in regenerative medicine.[29] Furthermore, the small size, excellent biocompatibility, low immunogenicity, and lack of risk for malignant transformation of small extracellular vesicles make them a highly promising cell-free therapeutic approach.

Interstitial cells derived from cardiac (ICs) have demonstrated a greater potential for secreting angiogenic factors compared to MSCs, particularly in hepatocyte growth factor, vascular endothelial growth factor (VEGF), and platelet-derived growth factor (PDGF) in our previous studies.[30–32] Furthermore, therapeutic approaches based on small extracellular vesicles derived from ICs (IC-sEV) have yet to be extensively validated in animal models of hindlimb ischemia. In this study, we hypothesized that IC-sEV possess superior angiogenic properties. To validate this hypothesis, we treated endothelial cells with IC-sEV that were successfully isolated and compared their impact on the gene expression of angiogenic factors relative to small extracellular vesicles secreted by adipose stem cells (ASC-sEV). We also investigated the paracrine actions of IC-sEV on endothelial cells *in vitro*. Additionally, we established a hindlimb ischemia animal model to evaluate the therapeutic effects of IC-sEV on ischemic mice and explore their underlying mechanisms of action.

2. Experimental

2.1. Cell culture

ICs were provided by Young Il Yang MD (Paik Institute for Clinical Research, Inje University College of Medicine, Busan, Republic of Korea). ICs were cultured in growth media consisting of Dulbecco's modified Eagle's medium (DMEM)-F12 (1 : 1), 10% fetal bovine serum, 10 ng mL^{-1} epidermal growth factor, 10 ng mL^{-1} insulin like growth factor, 2 ng mL^{-1} basic fibroblast growth factor (bFGF), and 1% antibiotic-antimycoplasmic reagent, with the media being changed every 3 days. Human umbilical vein endothelial cells (HUVECs) were purchased from Lonza (Basel, Switzerland) and cultured in EGM-2(Lonza) by changing the media every other day.

2.2. Isolation and purification of IC-sEV

Reduced serum media were conditioned by ICs for 3 days and collected. IC-sEV were isolated from the conditioned media by a sequential centrifugation method with minor modifications.[32] The conditioned media was centrifuged at 2000*g* for 20 min at 4 °C followed by centrifugation at 5000*g* for 30 min at 4 °C. To obtain the IC-sEV pellet, the supernatant was ultra-centrifuged at 10 000*g* for 70 min at 4 °C using Optima L-70K ultracentrifuge (Beckman Coulter, Brea, CA, USA). The IC-sEV pellet was washed with phosphate buffered saline (PBS) by ultra-centrifugation at 10 000*g* for 70 min at 4 °C. Extra liquid was removed and the pellet which contains IC-sEV was resuspended in PBS and the IC-sEV suspension was stored at −70 °C for further use. The IC-sEV concentration was measured using a BCA kit (Solarbio, Beijing, China).

2.3. Transmission electron microscopy (TEM)

The images of IC-sEV were acquired with a transmission electron microscope (Hitachi HT7700, Japan). The IC-sEV suspension was dropped onto a 200-mesh copper grid to adsorb for 2 min. After removing the droplet using filter paper, 2% phosphotungstic acid was applied to the grid for 2 min to negatively stain the sample, which was then allowed to dry naturally at room temperature. The grid was observed at an acceleration voltage of 80 kV equipped with an AMT 16-megapixel digital camera.

2.4. Nanoparticle tracking analysis (NTA)

The particle size distribution of IC-sEV was determined using a NTA instrument (Particle Metrix-PMX). First, IC-sEV were thoroughly mixed with filtered PBS in a centrifuge tube. Before injecting the diluted IC-sEV solution into the sample chamber, a 1 mL sterile syringe was used to draw and inject fresh Milli-Q water into an instrument at a uniform speed to flush the tubing. Subsequently, the diluted IC-sEV solution was injected at a constant rate. The NTA instrument irradiated the injected IC-sEV solution with a laser and utilized the properties of light scattering and Brownian motion to detect and analyze the particle size distribution of IC-sEV in the suspension in real time.

2.5. Protein extraction and western blotting

ICs and IC-sEV were lysed, respectively, with RIPA buffer (Rockland, PA, USA) containing a protease inhibitor (Quartett, Berlin, Germany), followed by subsequent centrifugation at 14 000*g* for 10 min at 4 °C. The supernatants were mixed with 4× Laemmli sample buffer and boiled at 95 °C for 5 min. The total protein (18 μg) was electrophoresed in 12% (w/v) sodium dodecyl sulfate polyacrylamide gels at 80 V for 15 min and then 100 V for 80 min. The proteins in the gel were transferred onto 0.2 μm polyvinylidene difluoride membranes (Bio-rad) using a Trans-blot Turbo Transfer System (Bio-rad) and blocked with 5% non-fat milk/0.05% Tween 20 in tris-buffered saline (TBS) for 1 h at room temperature. The membranes were probed with the following primary antibodies overnight at 4 °C: monoclonal rabbit anti-Hsp70 (1 : 1000, System Biosciences, CA, USA), monoclonal rabbit anti-CD9 (1 : 1000, System Biosciences, CA, USA), and monoclonal rabbit anti-CD81 (1 : 1000, System Biosciences, CA, USA). Following this, the membranes were washed three times with TBS and then incubated with horseradish peroxidase-conjugated goat anti-rabbit IgG (1 : 20 000, System Biosciences, CA, USA) for 1 h at room temperature. After three additional washes, the blots on the membrane were developed using the ChemiDoc™ MP (Bio-rad).

2.6. PKH67 labeling and internalization of IC-sEV

PKH67 dyes, which contain long fatty acid chains that insert spontaneously into cell membranes, were used to label IC-sEV. The specific procedure is as follows: IC-sEV were labeled with 2 μM PKH67 dyes (Sigma-Aldrich, St Louis, MO, USA) for 5 min at room temperature followed by quenching with 1% bovine serum albumin/PBS to stop the reaction. The labeled IC-sEV were washed with PBS by ultra-centrifugation at 100 000*g* for 70 min at 4 °C. The images were observed under a fluorescence microscope (Observer7 Apotome; Carl Zeiss, Gottingen, Germany) at 0 h, 6 h, and 24 h of IC-sEV treatment on HUVECs. The nuclei of HUVECs were stained with 4,6-diamino-2-phenylindole (DAPI, Thermo Fisher Scientific, Waltham, USA). To assess the internalization efficiency of IC-sEV in HUVECs, a flow cytometer was used for detection at 24 h.

2.7. RNA extraction and the quantitative real-time PCR (qRT-PCR)

HUVECs were seed into 6-well plates. After 24 h, the medium was replaced with growth medium containing 20 μg mL^{-1} IC-sEV or 20 μg mL^{-1} ASC-sEV, or without these small extracellular vesicles, and RNA isolation was conducted after 24 h. The total RNA was extracted using the TRIzol® reagent (Ambion) according to the manufacturer's instruction. Based on the RNA concentration determined using a NanoDrop 2000 spectrophotometer (Thermo Scientific, IL, USA), 1 μg total RNA from each sample was used for cDNA synthesis by using an iScript™ cDNA Synthesis Kit (Bio-Rad Laboratories, CA, USA). The yield and quality of cDNA were assessed using a NanoDrop 2000 spectrophotometer and 50 μg of cDNA was used to perform the qRT-PCR. The mRNA levels of angiogenic growth factors were determined using a CFX96™ Real-Time PCR detection system (Bio-Rad) with iQ™ SYBR Green Supermix (Bio-Rad). The sequences of the primers were as follows: VEGF-A, forward 5′-GGA GTA CCC CGA TGA GAT AGA GT-3′, reverse 5′-CTA TGT GCT GGC TTT GGT GAG-3′; bFGF, forward 5′-CCG TTA CCT GGC TAT GAA GG-3′, reverse 5′-ACT GCC CAG TTC GTT TCA GT-3′; PDGF-B, forward 5′-CCA TTC CCG AGG AGC TTT ATG-3′, reverse 5′-CAG CAG GCG TTG GAG ATC AT-3′; Ang-1, forward 5′-GAA GGG AAC CGA GCC TAT TC-3′, reverse 5′-GCT CTG TTT TCC TGC TGT CC-3′; GAPDH, forward 5′-CAT GTT CGT CAT GGG GTG AAC CA-3′, reverse 5′-AGT GAT GGC ATG GAC TGT GGT CAT-3′. Target genes were amplified by the following conditions: 95 °C for 3 min, followed by 40 cycles of 95 °C for 10 s and 59 °C for 30 s. Each relative gene expression was normalized by GAPDH as a reference gene and quantified by the $2^{-\Delta\Delta Ct}$ method. The results were presented as fold-changes relative to the control.

2.8. Cell proliferation assay

HUVECs (1.0×10^3 cells per cm^2) were seeded onto 96-well plates and cultured in different concentrations of IC-sEV (0, 10, 20, 30, 40, and 50 μg mL^{-1}) for 72 h. To analyze the cell viability at 24 h and 72 h of incubation, HUVECs treated IC-sEV were incubated in CCK-8 solution for 100 min at 37 °C and the absorbance at 450 nm was measured using a microplate multireader (Tecan, Mannedorf, Switzerland).

2.9. Wound healing assay

To assess the effect of IC-sEV on cell migration ability, a wound healing assay was conducted. HUVECs were seeded onto 24-well plates and incubated with growth media. When reached 80% confluency, the cells were treated with 10 μg mL^{-1} mitomycin C for 2 h to arrest cell proliferation. And then, the cell monolayer was scratched vertically to create a gap using a sterile 200 μL pipette tip and washed with pre-warmed PBS. 20 μg mL^{-1} IC-sEV in EGF-2 were treated and the migration into the gap was observed with a bright field microscope (Observer7; Carl Zeiss, Oberkochen, Germany). The wound closure rate (%) was calculated using the following equation: $(A_0 - A_{12})/A_0 \times 100\%$, where A_0 and A_{12} stand for the remaining gap area at 0 and 12 h of incubation, respectively.

2.10. Tube formation assay

96-well plates were pre-coated with 70 μL of matrigel (Corning, NY, USA) and incubated at 37 °C for 30 min for complete gelation of matrigel. 2.5×10^4 cells per well of HUVECs stained

with 2 μM calcein–AM (Invitrogen, CA, USA) were plated onto the matrigel and HUVECs were treated the reduced serum media with or without IC-sEV. After 8 h of incubation, capillary-like tube networks were observed under a fluorescence microscope (Carl Zeiss, Gottingen, Germany). The degree of tube formation was determined by the total tube length per total area and the number of branch points per total area.

2.11. Murine hindlimb ischemia model and treatment

In vivo experiments were performed with male BALB/c nude mice (7 weeks old), purchased from the Beijing Vital River Laboratory Animal Technology (China). All animal procedures were reviewed and approved by the Animal Ethical and Welfare Committee of Tianjin Medical University and conformed to the feeding requirements of the International Guidelines for the Care and Use of Laboratory Animals. The hindlimb ischemia model was induced as described previously.[33] In brief, the mice were anesthetized using 1% pentobarbital sodium (75 mg kg^{-1}). The femoral artery of the left hindlimb was ligated and severed at two locations after separating the femoral artery from the vein and nerve, namely the distal branch of the femoral artery and the femoral artery located between the superficial iliac circumflex artery and the deep femoral artery. On the day after ischemic surgery, these nude mice were randomly divided into 2 groups: PBS group and IC-sEV group. In the IC-sEV treatment group, 100 μg of sEV dissolved in 100 μL PBS were injected into 3 different sites near the ligation site. The PBS group received an equal volume of PBS. The sham group underwent the same operation except for ligation and severing of the femoral artery.

2.12. Assessment of ischemic limb functional performance

Blood perfusion in ischemic or normal limbs was measured using a laser doppler perfusion imager system (Perimed AB, Sweden) on the first postoperative day and on days 7, 14, 21, and 28 after treatment. The blood perfusion rate of the left ischemic limb (%) = blood flow of the ischemic limb/blood flow of the normal limb × 100%. The limb function was assessed using a clinical score: grade 0 indicated flexing the toes to resist gentle traction on the tail; grade 1 indicated plantar flexion; grade 2 indicated no dragging but no plantar flexion; and grade 3 indicated the dragging of the foot.[34] Tissue damage was also assessed with a grading system: Grade 0 indicated no difference from the right hindlimb; grade 1 indicated mild discoloration; grade 2 indicated moderate discoloration; grade 3 indicated severe discoloration, subcutaneous tissue loss, or necrosis; and grade 4 indicated amputation.[35] The limb status was rated on day 28 post-injection, with categories including limb salvage, foot necrosis, and limb loss.[36]

2.13. Histology analysis

After 28 days of treatment, the nude mice were anesthetized, and the gastrocnemius muscles from the ischemic limbs and main organs were collected. The tissues were fixed in 4% paraformaldehyde and embedded in either paraffin or the OTC compound (Sakura Finetek, USA). Sections of 6 μm thickness were cut from the embedded tissues for subsequent immunostaining. To assess the effects of IC-sEV on ischemic limbs, immunofluorescence staining was performed to detect CD31, α-smooth muscle actin (α-SMA), CD68, and apoptotic cells in the ischemic muscles. Observations were made using a confocal microscope (Olympus FV1000, Japan), and quantifications were measured with Image J software. Additionally, tumor necrosis factor alpha (TNF-α) in the ischemic muscles was identified through immunohistochemical staining and images were taken with a microscope (Olympus BX51, Japan), with analyzed using IPP software. Hematoxylin and eosin (H&E) staining was utilized to evaluate inflammatory infiltration, while Masson's staining assessed the degree of fibrosis in the muscle tissue. The area ratio was analyzed using Image J software. To determine the safety of IC-sEV locally injection, main organ sections were stained with H&E.

2.14. Statistical analysis

All data were presented as mean ± SEM, statistical analysis of two independent groups was performed using Student's *t*-test, and one-way ANOVA was used for comparing multiple groups. All analyses were conducted using GraphPad 8.0 (GraphPad Prism Software, USA). $P < 0.05$ indicated a statistically significant difference.

3. Results and discussion

3.1. Isolation and characterization of IC-sEV

As described previously in the Experimental section, IC-sEV were isolated from the culture medium of ICs by ultracentrifugation. We next employed various methods to study the characterization of IC-sEV. The morphology of IC-sEV was examined using TEM, which revealed oval shape vesicles, as depicted in Fig. 1A. The NTA indicated that the particle size of IC-sEV is concentrated around 95.5 nm (Fig. 1B), suggesting a relatively homogeneous population of sEV within the sample. These results are consistent with the small extracellular vesicle characteristics reported.[21] During the formation of small extracellular vesicles, the parent cells encapsulate active components such as proteins and RNA inside the vesicles or attach them to the vesicle membrane.[37] Western blotting of IC-sEV and ICs also confirmed that IC-sEV exhibited higher levels of Hsp70, CD9 and CD80 compared with the IC lysate (Fig. 1C), highlighting the selective incorporation of proteins into these vesicles.

3.2. Internalization of IC-sEV

Studies have shown that small extracellular vesicles can enter recipient cells through multiple pathways, including non-specific mechanisms such as macropinocytosis and phagocytosis, as well as receptor-mediated endocytosis and pH-dependent fusion with the plasma membrane.[38] To confirm whether IC-sEV can be internalized by endothelial cells, IC-sEV were stained with PKH67 (green) and incubated with HUVECs *in vitro*. The fluorescence imaging results indicated that distinct green fluorescent particles appeared in the cells, almost exclusively distributed in the cytoplasm, after co-incubation

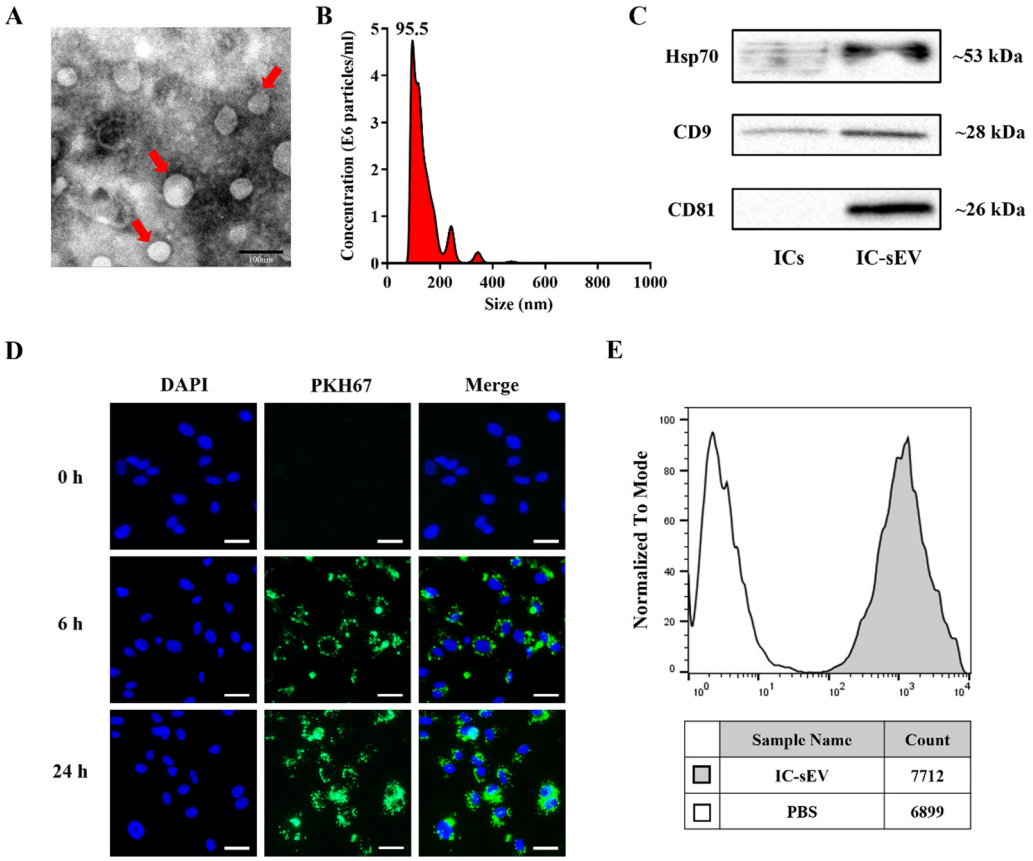

Fig. 1 IC-sEV characteristics and internalization. (A) Representative transmission electron microscopy image of IC-sEV (scale bar = 100 nm). (B) The particle size distribution of IC-sEV determined by NTA. (C) Western blotting analysis of Hsp70, CD9 and CD81 in ICs and IC-sEV. (D) Confocal microscopy images of PKH67-labeled IC-sEV (green) internalization by HUVECs at 0, 6, and 24 hours, with HUVEC nuclei (blue) stained by DAPI (scale bar = 100 μm). (E) Flow cytometry analysis of the internalization rate of IC-sEV by HUVECs for 24 h.

with IC-sEV for 6 h; when the incubation time extended to 24 h, the labeled IC-sEV had entered the cell nucleus (Fig. 1D). As shown in Fig. 1E, the flow cytometry results indicated that after co-culturing with HUVECs for 24 h, 99.9% of the cells had internalized IC-sEV labeled with PKH67. These data suggested that the IC-sEV can be internalized by endothelial cells and the uptake of PKH67-labeled IC-sEV is time-dependent over a certain time range, suggesting that uptake efficiency is optimized by regulating the incubation time of IC-sEV with cells.

3.3. Increased expression proangiogenic factors in IC-sEV

To compare the effects of IC-sEV and small extracellular vesicles derived from stem cells on the promotion of angiogenic factors, HUVECs were treated with IC-sEV and ASC-sEV for 24 h, and the expression levels of mRNA related to angiogenesis factors in HUVECs were detected by the qRT-PCR (Fig. 2). ASC-sEV showed an increase in the expression levels of bFGF in cells, which were 1.36-fold higher than those in the PBS group. In contrast, the expression levels of VEGF, Ang-1 and PDGF were not significantly different from those in the PBS group. Compared to the PBS group, treatment with IC-sEV significantly increased the gene expression levels of VEGF, bFGF, and Ang-1 in HUVECs by 1.53-fold, 1.51-fold, and 1.72-fold, respectively. In addition, the expression of PDGF in cells was 1.61-fold higher than that observed in ASC-sEV. The results of the qRT-PCR experiments indicated that IC-sEV significantly upregulated the gene expression levels of angiogenesis-related factors in HUVECs compared to the ASC-sEV group.

Accumulating evidence underscores the pivotal role of angiogenic factors and their signaling pathways in neovascularization within ischemic diseases.[39] For instance, Ang-1 binds to the Tie2 receptor on mural cells, modulating interactions between endothelial cells and mural cells to enhance new vascular wall integrity, reduce vascular leakage, and ultimately facilitate the formation of stable and mature vessels.[40,41] The increased expression of these angiogenic factors by IC-sEV highlights its potential to promote neovascularization. To further substantiate these findings, our subsequent experiments will validate the therapeutic efficacy of IC-sEV both *in vitro* and *in vivo*, providing comprehensive evidence of its potential as a novel treatment strategy for CLI.

3.4. Enhanced paracrine actions of IC-sEV *in vitro*

Small extracellular vesicles carry a variety of bioactive molecules, such as proteins, lipids, and nucleic acids, which give the extracellular vesicles specific biological properties. Once released,

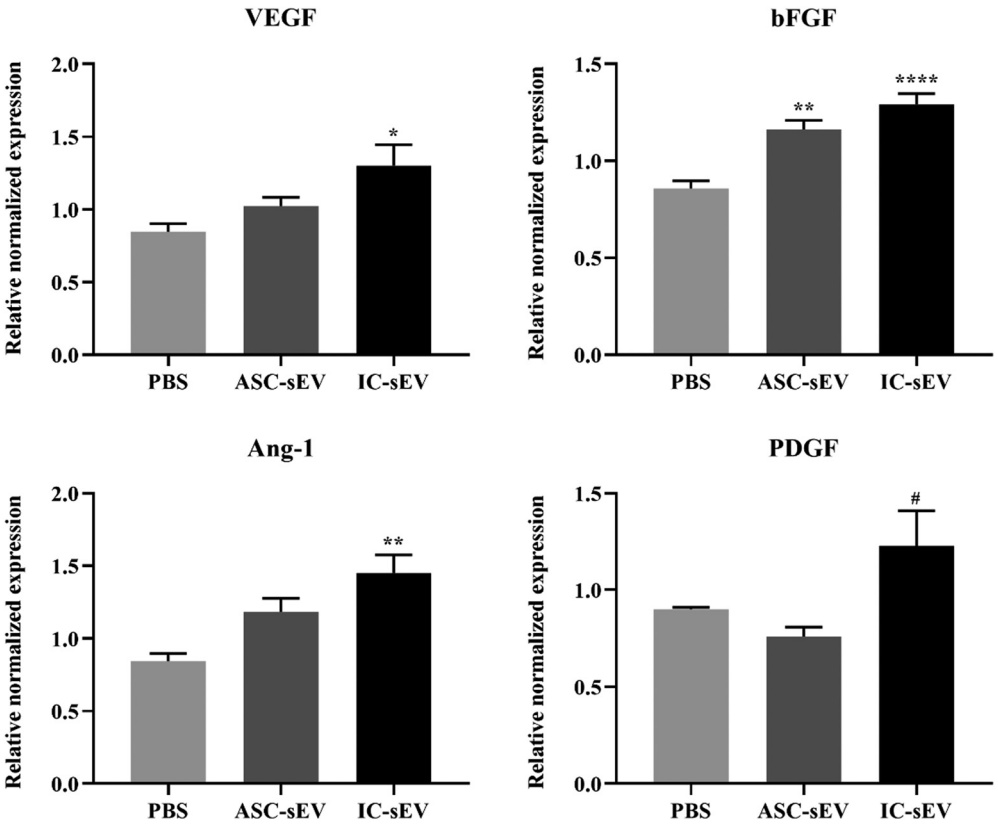

Fig. 2 Effects of IC-sEV and ASC-sEV on the expression levels of VEGF, bFGF, PDGF and Ang-1 on HUVECs (n = 5, *$p < 0.05$, **$p < 0.01$, ***$p < 0.001$ compared with PBS; $^{\#}p < 0.05$ compared with ASC-sEV).

small extracellular vesicles can enter the surrounding cells or distant cells to produce a spectrum of biological effects.[42] To assess the proangiogenic potential of IC-sEV *in vitro*, we performed a cell proliferation assay, a wound healing assay and a tube formation assay on HUVECs. The CCK-8 assay results demonstrated that IC-sEV promoted endothelial cell proliferation at 24 h and 72 h, with a more significant effect observed at 72 h (Fig. 3A), indicating that the longer the co-culture time with IC-sEV, the higher the cell activity. After HUVECs were treated with IC-sEV for 12 h, wound healing ability was evaluated by observing cell migration. The results showed that the wound closure ratio in the IC-sEV group (77.18 ± 4.27%) was markedly higher than that in the PBS group (48.87 ± 2.63%) (Fig. 3B and C). For the tube formation assay, the total tube length was significantly increased in the IC-sEV group (10.16 ± 0.47 mm mm^{-2}), compared to the PBS group (8.59 ± 0.22 mm mm^{-2}), and the number of branch points in the IC-sEV group was 1.4-fold that of the PBS group (Fig. 3E and F). These results suggested that IC-sEV enhanced endothelial cell proliferation, wound healing and tube formation abilities. In conclusion, these findings provide a strong foundation for further exploring the therapeutic potential of IC-sEV *in vivo*.

3.5. Improved blood perfusion and promoted salvage of ischemic hindlimb in IC-sEV

To investigate the effect of IC-sEV transplantation on blood perfusion in ischemic limbs of mice, we established ischemic hindlimb nude mice models. On the first day after surgery, 100 μg of IC-sEV was intramuscularly injected into the left ischemic hindlimb performing two excisions. After 28 days, there were striking differences in blood recovery, limb salvage, and limb function between the ischemic hindlimb mice treated with IC-sEV and the PBS group. Blood perfusion images and rates were measured using a Laser Doppler on days 0, 7, 14, 21, and 28 (Fig. 4A and B). At day 0, both the IC-sEV group and the PBS group showed similarly low levels of blood perfusion. After one week of treatment, the blood perfusion rate of the ischemic limbs in the IC-sEV group (43.45 ± 6.75%) was significantly higher than that in the PBS group (19.72 ± 5.20%). Over the following three weeks, both groups showed increases in blood perfusion rates, but the IC-sEV group exhibited a markedly faster recovery. By the end of the fourth week, the blood perfusion rate in the IC-sEV group reached approximately 80%, whereas the self-recovery rate in the PBS group was only 46%. These results demonstrate the therapeutic efficacy of locally administered IC-sEV in promoting blood flow recovery in ischemic limbs.

On 28 days after treatment, the recovery of the ischemic limbs in nude mice was scored, as shown in Fig. 4C. 87.5% of the nude mice underwent limb loss and 12.5% suffered foot necrosis in the PBS group. In contrast, the IC-sEV group showed a significant increase in hindlimb salvage, with 50% showing no limb loss or necrosis at day 28. To further evaluate the

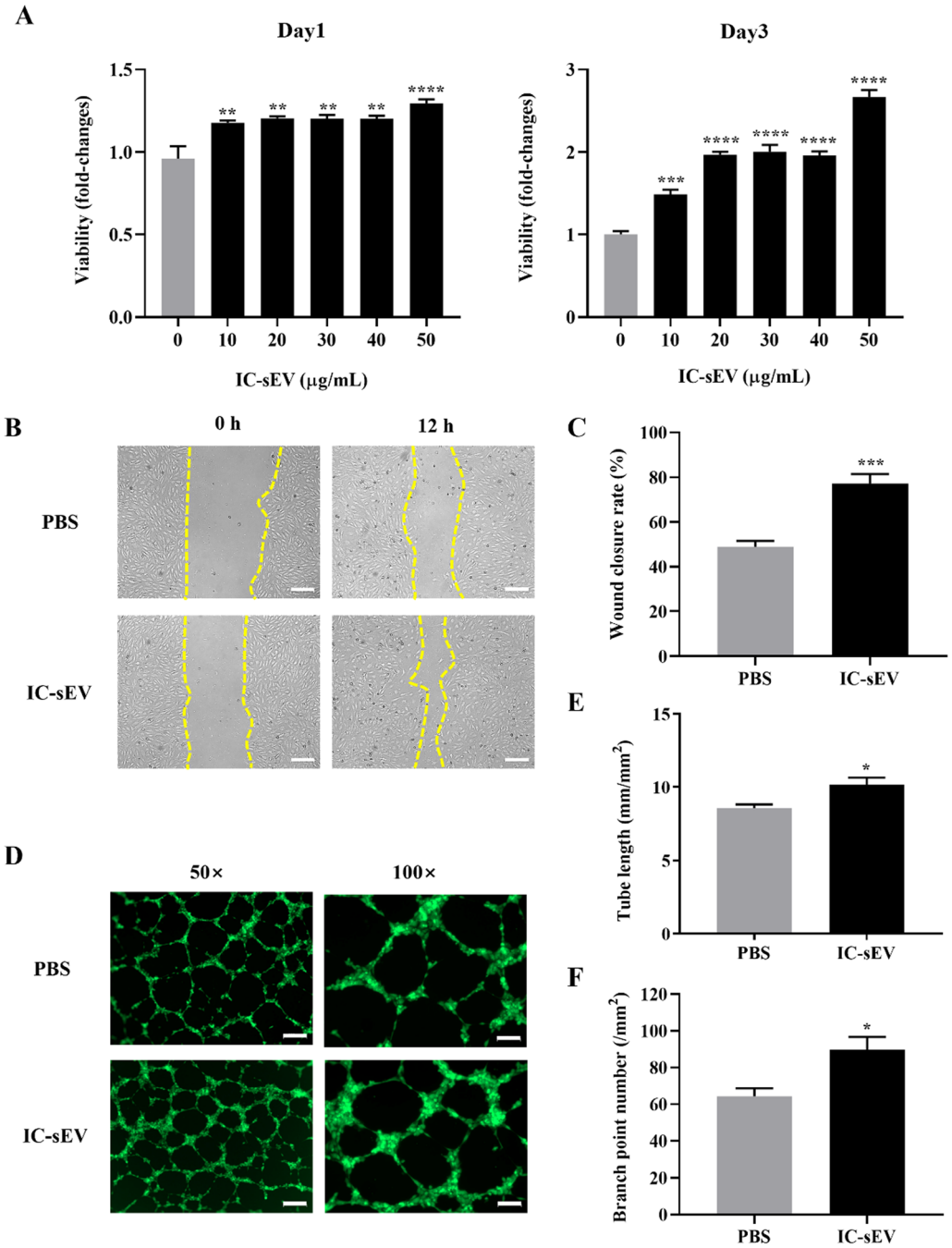

Fig. 3 Paracrine effects of IC-sEV on HUVECs. (A) Effects of different concentrations of IC-sEV on the proliferation capacity of HUVECs on day 1 and day 3 (n = 3, $^{**}p < 0.01$, $^{***}p < 0.001$, $^{****}p < 0.0001$ compared to 0 μg mL^{-1} IC-sEV). (B) Representative images of the wound healing assay of HUVECs treated with 20 μg mL^{-1} IC-sEV for 0 h and 12 h (scale bar = 200 μm). (C) Quantitative analysis of the wound healing assay at 12 h (n = 5, $^{***}p < 0.001$ compared to the PBS group). (D) Confocal microscopy images of HUVECs treated with 20 μg mL^{-1} IC-sEV at different magnifications for 8 h (scale bar = 200 μm under 50× and scale bar = 100 μm under 100×). (E) Quantitative analysis of the tube length in the tube formation assay (n = 5). (F) Quantitative assessment of branch points number in the tube formation assay (n = 5, $^{*}p < 0.05$ compared with the PBS group).

effects of local transplantation of IC-sEV on motor capacity and tissue damage of ischemic limbs in nude mice, we scored ambulatory impairment and tissue damage on days 0, 7, 14, 21, and 28 after IC-sEV transplantation (Fig. 4D and E). At day 7, the limb function of the IC-sEV group recovered significantly compared with that of the PBS group and continued to improve. The ambulatory impairment and tissue damage score in the IC-sEV group was significantly reduced compared with the PBS group at day 28. These data demonstrated that IC-sEV promoted the recovery of ischemic limb functions.

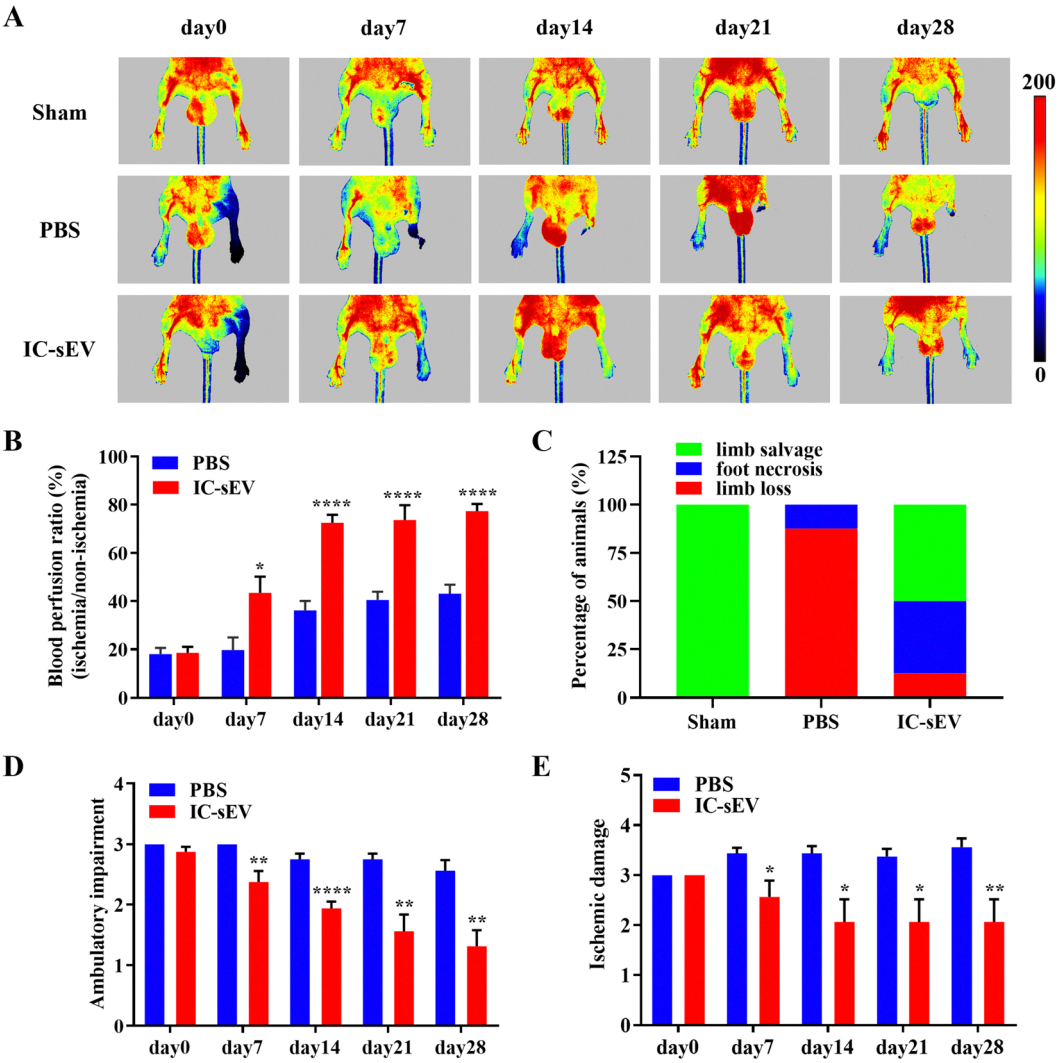

Fig. 4 IC-sEV improves blood perfusion and facilitates recovery in ischemic hindlimbs of nude mice. (A) Representative Laser Doppler perfusion images from nude mice treated IC-sEV and PBS on days 0, 7, 14, 21, and 28. The transition of the color scale from "dark to bright" within the images indicates an increase in blood perfusion. (B) Quantitative analysis of blood perfusion ratio at each time point. (C) Percentage distributions of limb loss, foot necrosis, and limb salvage. (D) Ambulatory impairment scores of nude mice treated IC-sEV and PBS at each time point. (E) Ischemic damage scores of nude mice treated IC-sEV and PBS at each time point (n = 8, *$p < 0.05$, **$p < 0.01$, ****$p < 0.0001$ compared to PBS).

3.6. Exerted pro-angiogenic effects of IC-sEV *in vivo*

Muscle recovery following ischemia is primarily contingent upon angiogenesis, a process that enables the exchange of nutrients and oxygen. To elucidate the therapeutic mechanism of IC-sEV, we performed CD31 and α-SMA immunofluorescence staining on gastrocnemius muscle sections 28 days after IC-sEV transplantation. These markers specifically identify endothelial cells and smooth muscle cells within the blood vessels, indicative of angiogenesis. The PBS group exhibited minimal expression of CD31 and α-SMA, while a marked elevation in fluorescence intensity was observed in the IC-sEV group (Fig. 5A). The average positive staining area percentage was 0.27 ± 0.02% for CD31 and 0.73 ± 0.02% for α-SMA in the PBS group, whereas the IC-sEV group displayed significantly higher averages of 0.57 ± 0.03% for CD31 and 1.49 ± 0.07% for α-SMA (Fig. 5B and C). Notably, the expression levels of both CD31 and α-SMA in the IC-sEV group were approximately twice those of the PBS group. Collectively, these findings indicated that IC-sEV may achieve therapeutic effects by promoting new angiogenesis at the ischemic site, which may be attributed to the angiogenesis-related factor mRNA in IC-sEV, such as VEGF mRNA.[38,43] Once cells take up IC-sEV, the VEGF mRNA is transferred to recipient cells and translated into VEGF.[44] Subsequently, VEGF is secreted extracellularly and binds to the VEGF receptor on the surface of endothelial cells, activating the PI3K-Akt pathway to promote endothelial cell proliferation, migration, and lumen formation.[45] However, the exact mechanisms underlying these effects of IC-sEV still require further research and exploration.

3.7. Suppressed inflammatory effects of IC-sEV *in vivo*

Under conditions of tissue ischemia and hypoxia, oxidative stress reactions are intensified, which may lead to the

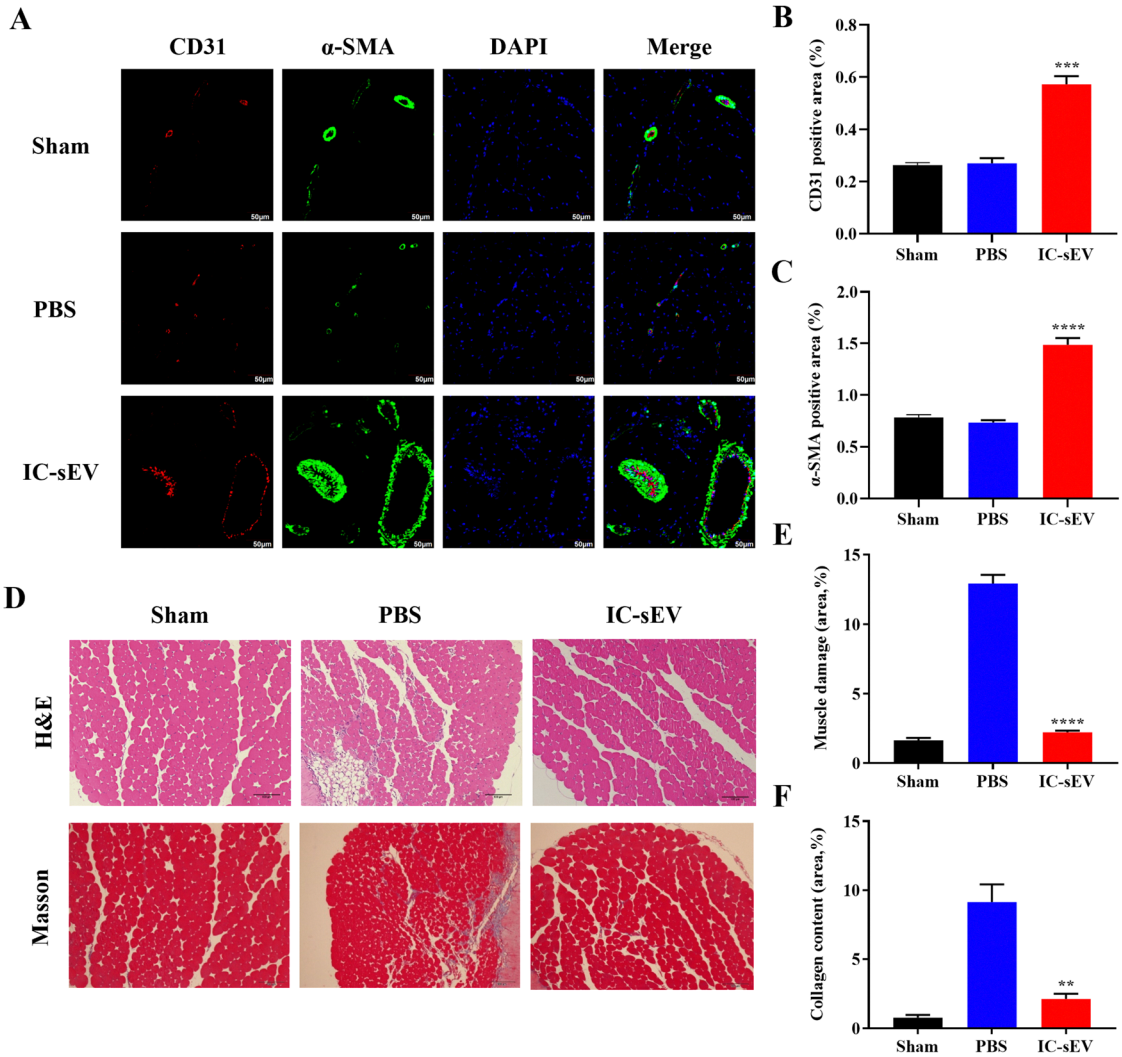

Fig. 5 IC-sEV enhances proangiogenic effects and tissue repair in ischemic hindlimb at 28 days after treatments (Note: the sham group (undergoing a surgical procedure without ligation and severing of the femoral artery), as a surgical control; the PBS group (ligation and severing of the femoral artery followed by 100 μL PBS injection), as a negative control). (A) Representative immunofluorescence images of CD31 (red) and α-SMA (green) in muscle tissues at 28 days after treatments, with co-stained nuclei (blue) (scale bar = 50 μm). (B) Quantitative analysis of CD31 staining intensity (n = 4). (C) Quantitative assessment of α-SMA staining intensity (n = 4). (D) Representative H&E staining and Masson staining images of muscle tissues (scale bar = 100 μm). (E) Quantification of the area of muscle damage in H&E staining sections (n = 4). (F) Quantification of the area of muscle fibrosis in Masson staining sections (n = 4, $^{**}p < 0.01$, $^{***}p < 0.001$ and $^{****}p < 0.001$ compared to PBS).

occurrence and exacerbation of inflammatory responses. Macrophages play a key role in this process, releasing pro-inflammatory cytokines such as TNF-α, IFN-γ and IL-6, which are crucial for the initiation and regulation of the inflammatory process.[46] Meanwhile, the clearance activities of immune cells at the site of inflammation may lead to apoptosis and destruction of the tissue structure. To determine if the muscles of the ischemic hindlimb exhibit degeneration and fibrosis following intramuscular injection of IC-sEV, muscle tissues were analyzed histologically. Staining images of muscle tissues in the IC-sEV group showed less muscle degeneration and significantly reduced collagen deposition compared to the PBS group (Fig. 5D). Additionally, ischemic muscle sections underwent immunostaining for TNF-α and CD68 on day 28. The IC-sEV treatment notably decreased macrophage and inflammatory cytokine infiltration compared to the PBS group (Fig. 6A and C). Quantification of the CD68 positive area was 0.72% ± 0.05% in the IC-sEV group, which was significantly lower than the 2.35% ± 0.31% in the PBS group (Fig. 6B). The positive area of TNF-α infiltration in the IC-sEV group was 4-fold less than that of the PBS group (Fig. 6D). Apoptosis in ischemic limb muscles was assessed using a TUNEL assay. The percentage of apoptotic cells in the PBS group was 1.5-fold higher than that in the IC-sEV group on day 28 (Fig. 7). Together, these data suggested the effectiveness of IC-sEV in reducing inflammatory responses, cell apoptosis and tissue fibrosis at the ischemic site. Given that small extracellular vesicles carry specific miRNAs from parent cells when released, such as miRNA-126, which can reduce the levels of pro-inflammatory factors TNF-α and IL-1β as well as oxidative factors (ROS) by targeting and inhibiting the

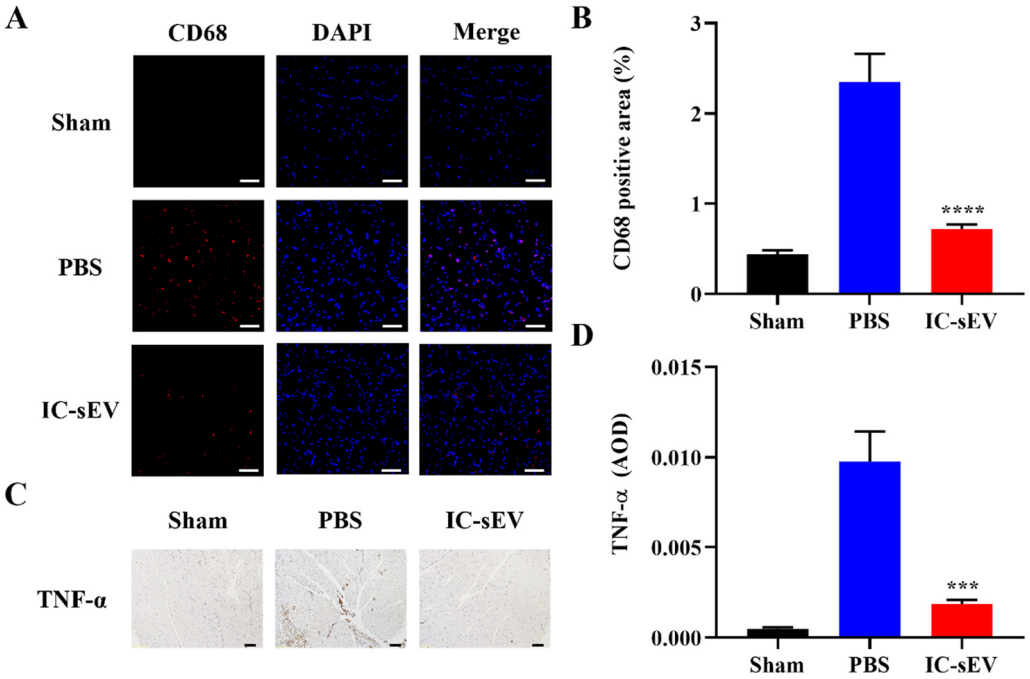

Fig. 6 IC-sEV attenuates inflammatory infiltration in limb ischemia nude mice at 28 days after treatments (Note: the sham group (undergoing a surgical procedure without ligation and severing of the femoral artery), as a surgical control; the PBS group (ligation and severing of the femoral artery followed by 100 μL PBS injection), as a negative control). (A) Representative images of CD68 immunofluorescence staining, indicating macrophage infiltration (red) in the ischemic muscle tissues, with nuclei counterstained (blue) (scale bar = 50 μm). (B) Quantitative analysis of CD68 positive areas (n = 10). (C) Representative immunohistochemical images of TNF-α expression (scale bar = 100 μm). (D) Quantification of the expression of TNF-α in the ischemic muscle (n = 10, ***$p < 0.001$ and ****$p < 0.001$ compared to PBS).

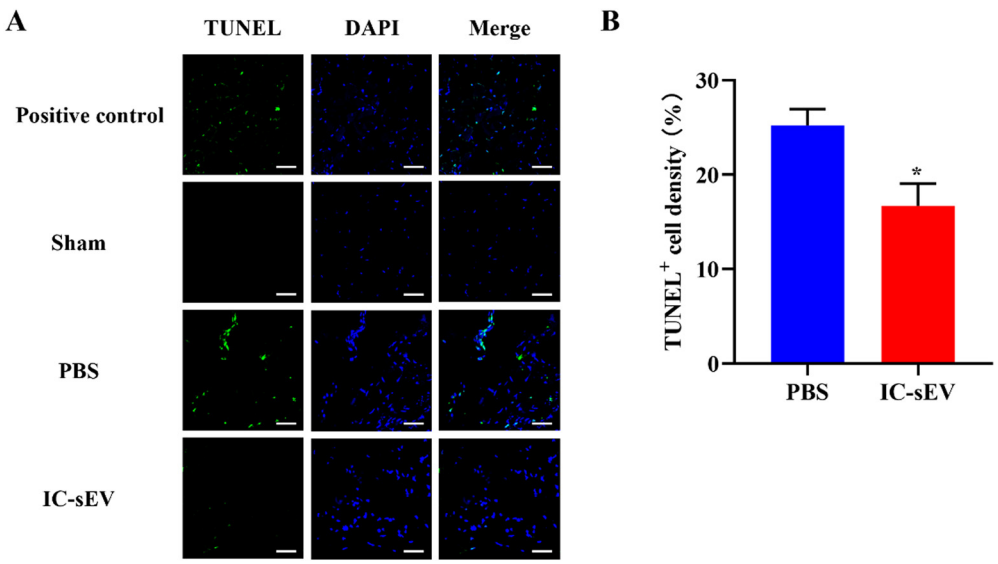

Fig. 7 IC-sEV reduces muscle injury in limb ischemia nude mice at 28 days after treatments. (A) Representative immunofluorescence images showing TUNEL staining (green) in muscle tissues, indicating apoptotic cells, with nuclei counterstained (blue) (scale bar = 50 μm). (B) Quantification of the ratio of TUNEL positive cells at day 28 (n = 4, *$p < 0.05$ compared to PBS).

expression of the S1PR2 protein.[47] And in various ischemic diseases, it participates in endothelial cell migration, cytoskeleton recombination and the regulation of capillary network stability through the mechanism mediated by the PI3K/Akt/eNOS signaling pathway.[48–50] These mechanisms likely contribute to the pro-angiogenic and anti-inflammatory effects of IC-sEV. However, given the complex composition of IC-sEV, its overall effects may result from the synergistic action of multiple components. Further research is needed to confirm the exact mechanism of IC-sEV action.

Histopathological changes in the major visceral organs were observed to evaluate the systemic toxicity of each treatment. The organs treated with IC-sEV showed a similar natural organization structure to the sham group, as depicted in Fig. S1 (ESI†). The results showed that local injection of IC-sEV does not exert toxicity on the organs of nude mice.

4. Conclusions

In summary, IC-sEV have exhibited a more potent effect on angiogenic factors than ASC-sEV and the pro-angiogenic potential of IC-sEV has been validated by promoting endothelial cells' proliferation, migration, and tube formation. Furthermore, the transplantation of IC-sEV into ischemic tissues has been shown to significantly enhance the blood perfusion rate of ischemic limbs and promote the recovery of motor functions in these limbs. Additional findings reveal that IC-sEV fostered neovascularization, reduced cellular apoptosis, and decreased inflammatory infiltration as well as fibrosis. The local transplantation of IC-sEV holds promise as a novel cell-free therapeutic strategy, providing an effective alternative to cell therapy for ischemic tissue injury.

Author contributions

Nana Wang: writing – review and editing, writing – original draft, methodology, investigation, formal analysis, data curation, and conceptualization. Xing Pei: writing – review and editing, supervision, methodology, investigation, and conceptualization. Yaxuan Feng: investigation and validation. Lu Sun: conceptualization and writing – review and editing. Chao Zhang: conceptualization and writing – review and editing. Seungjin Lee: conceptualization, writing – review and editing, and funding acquisition. Fei Yu: conceptualization, writing – review and editing, and funding acquisition.

Conflicts of interest

The authors declare that they have no known competing financial interests or personal relationships that could have appeared to influence the work reported in this paper.

Data availability

All data that support the findings of this study are available upon request by contact with the corresponding author.

Acknowledgements

This work was supported by grants from the Science & Technology Development Fund of Tianjin Education Commission for Higher Education (2019KJ178).

References

1 K. L. McGinigle, Peripheral Vascular Disease, *Prim. Care - Clin. Off. Prac.*, 2024, **51**, 83–93.
2 Y. Dong, Y. Liu, P. Cheng, H. Liao, C. Jiang, Y. Li, S. Liu and X. Xu, Lower limb arterial calcification and its clinical relevance with peripheral arterial disease, *Front. Cardiovasc. Med.*, 2023, **10**, 1271100.
3 D. Mandaglio-Collados, F. Marín and J. M. Rivera-Caravaca, Peripheral artery disease: Update on etiology, pathophysiology, diagnosis and treatment, *Med. Clin.*, 2023, **161**, 344–350.
4 S. S. Signorelli, E. Marino, S. Scuto and D. Di Raimondo, Pathophysiology of Peripheral Arterial Disease (PAD): A Review on Oxidative Disorders, *Int. J. Mol. Sci.*, 2020, **21**, 4393.
5 S. R. Levin, N. Arinze and J. J. Siracuse, Lower extremity critical limb ischemia: A review of clinical features and management, *Trends Cardiovasc. Med.*, 2020, **30**, 125–130.
6 J. Golledge, Pathology, Progression, and Emerging Treatments of Peripheral Artery Disease-Related Limb Ischemia, *Clin. Ther.*, 2023, **45**, 1077–1086.
7 H. Wu, P. Ye, Y. Chen, Y. Li, C. Cai and P. Lv, The current state of endovascular intervention for critical limb ischemia: A systematic review, *Vasc. Invest. Ther.*, 2021, **4**, 46–53.
8 R. Martini and F. Ghirardini, Patients with critical limb ischemia (CLI) not suitable for revascularization: The ''dark side'' of CLI, *Vasc. Invest. Ther.*, 2021, **4**, 87–94.
9 J. Golledge, Update on the pathophysiology and medical treatment of peripheral artery disease, *Nat. Rev. Cardiol.*, 2022, **19**, 456–474.
10 G. T. Park, J. K. Lim, E. B. Choi, M. J. Lim, B. Y. Yun, D. K. Kim, J. W. Yoon, Y. G. Hong, J. H. Chang, S. H. Bae, J. Y. Ahn and J. H. Kim, Transplantation of adipose tissue-derived microvascular fragments promotes therapy of critical limb ischemia, *Biomater. Res.*, 2023, **27**, 70.
11 M. Rojas-Torres, L. Beltrán-Camacho, A. Martínez-Val, I. Sánchez-Gomar, S. Eslava-Alcón, A. Rosal-Vela, M. Jiménez-Palomares, E. Doiz-Artázcoz, M. Martínez-Torija, R. Moreno-Luna, J. V. Olsen and M. C. Duran-Ruiz, Unraveling the differential mechanisms of revascularization promoted by MSCs & ECFCs from adipose tissue or umbilical cord in a murine model of critical limb-threatening ischemia, *J. Biomed. Sci.*, 2024, **31**, 71.
12 S. Fukuda, S. Hagiwara, H. Okochi, N. Ishiura, T. Nishibe, R. Yakabe and H. Suzuki, Autologous angiogenic therapy with cultured mesenchymal stromal cells in platelet-rich plasma for critical limb ischemia, *Regener. Ther.*, 2023, **24**, 472–478.
13 G. Arderiu, A. Civit-Urgell and L. Badimon, Adipose-Derived Stem Cells to Treat Ischemic Diseases: The Case of Peripheral Artery Disease, *Int. J. Mol. Sci.*, 2023, **24**, 16752.
14 L. V. Lozano Navarro, X. Chen, L. T. Giratá Viviescas, A. K. Ardila-Roa, M. L. Luna-Gonzalez, C. L. Sossa and M. L. Arango-Rodríguez, Mesenchymal stem cells for critical limb ischemia: their function, mechanism, and therapeutic potential, *Stem Cell Res. Ther.*, 2022, **13**, 345.

15 Y. Song, J. Yang, T. Li, X. Sun, R. Lin, Y. He, K. Sun, J. Han, G. Yang, X. Li, B. Liu, D. Yang, G. Dang, X. Ma, X. Du, B. Zhang, Y. Hu, W. Kong, X. Wang, H. Zhang, Q. Xu and J. Feng, CD^{34+} cell-derived fibroblast-macrophage cross-talk drives limb ischemia recovery through the OSM-ANGPTL signaling axis, *Sci. Adv.*, 2023, **9**, eadd2632.
16 T. Yamashita, H. Kawai, F. Tian, Y. Ohta and K. Abe, Tumorigenic Development of Induced Pluripotent Stem Cells in Ischemic Mouse Brain, *Cell Transplant.*, 2011, **20**, 883–892.
17 R. Alvites, M. Branquinho, A. C. Sousa, B. Lopes, P. Sousa and A. C. Maurício, Mesenchymal stem/stromal cells and their paracrine activity-immunomodulation mechanisms and how to influence the therapeutic potential, *Pharmaceutics*, 2022, **14**, 381.
18 N. S. Mabotuwana, L. Rech, J. Lim, S. A. Hardy, L. A. Murtha, P. P. Rainer and A. J. Boyle, Paracrine Factors Released by Stem Cells of Mesenchymal Origin and their Effects in Cardiovascular Disease: A Systematic Review of Pre-clinical Studies, *Stem Cell Rev. Rep.*, 2022, **18**, 2606–2628.
19 S. Bruno, S. Kholia, M. C. Deregibus and G. Camussi, The Role of Extracellular Vesicles as Paracrine Effectors in Stem Cell-Based Therapies, *Adv. Exp. Med. Biol.*, 2019, **1201**, 175–193.
20 C. Fusco, G. De Rosa, I. Spatocco, E. Vitiello, C. Procaccini, C. Frigè, V. Pellegrini, R. La Grotta, R. Furlan, G. Matarese, F. Prattichizzo and P. de Candia, Extracellular vesicles as human therapeutics: A scoping review of the literature, *J. Extracell. Vesicles*, 2024, **13**, e12433.
21 Y. Chen, Y. Zhao, Y. Yin, X. Jia and L. Mao, Mechanism of cargo sorting into small extracellular vesicles, *Bioengineered*, 2021, **12**, 8186–8201.
22 M. Negahdaripour, H. Owji, S. Eskandari, M. Zamani, B. Vakili and N. Nezafat, Small extracellular vesicles (sEVs): discovery, functions, applications, detection methods and various engineered forms, *Expert Opin. Biol. Ther.*, 2021, **21**, 371–394.
23 M. Mittelbrunn, C. Gutiérrez-Vázquez, C. Villarroya-Beltri, S. González, F. Sánchez-Cabo, M. Á. González, A. Bernad and F. Sánchez-Madrid, Unidirectional transfer of microRNA-loaded exosomes from T cells to antigen-presenting cells, *Nat. Commun.*, 2011, **2**, 282.
24 X. Zhou, Y. Jia, C. Mao and S. Liu, Small extracellular vesicles: Non-negligible vesicles in tumor progression, diagnosis, and therapy, *Cancer Lett.*, 2024, **580**, 216481.
25 C. Mas-Bargues, J. Sanz-Ros, N. Romero-García, J. Huete-Acevedo, M. Dromant and C. Borrás, Small extracellular vesicles from senescent stem cells trigger adaptive mechanisms in young stem cells by increasing antioxidant enzyme expression, *Redox Biol.*, 2023, **62**, 102668.
26 Y. Zhang, F. Zhen, Y. Sun, B. Han, H. Wang, Y. Zhang, H. Zhang and J. Hu, Single-cell RNA sequencing reveals small extracellular vesicles derived from malignant cells that contribute to angiogenesis in human breast cancers, *J. Transl. Med.*, 2023, **21**, 570.
27 I. Lee, Y. Choi, D. U. Shin, M. Kwon, S. Kim, H. Jung, G. H. Nam and M. Kwon, Small Extracellular Vesicles as a New Class of Medicines, *Pharmaceutics*, 2023, **15**, 325.
28 S. Munich, A. Sobo-Vujanovic, W. J. Buchser, D. Beer-Stolz and N. L. Vujanovic, Dendritic cell exosomes directly kill tumor cells and activate natural killer cells *via* TNF superfamily ligands, *Oncoimmunology*, 2012, **1**, 1074–1083.
29 D. Livkisa, T. H. Chang, T. Burnouf, A. Czosseck, N. T. N. Le, G. Shamrin, W. T. Yeh, M. Kamimura and D. J. Lundy, Extracellular vesicles purified from serum-converted human platelet lysates offer strong protection after cardiac ischaemia/reperfusion injury, *Biomaterials*, 2024, **306**, 122502.
30 X. Pei, J. Shin, H. Kim, N. Wang, C. Seo, M. Yoon, X. Chen, J. Gao, V. C. Yang, H. He and S. Lee, Cardiac-derived stem cell engineered with constitutively active HIF-1α gene enhances blood perfusion of hindlimb ischemia, *J. Ind. Eng. Chem.*, 2022, **105**, 210–221.
31 X. Pei, H. Kim, M. Lee, N. Wang, J. Shin, S. Lee, M. Yoon, V. C. Yang and H. He, Local delivery of cardiac stem cells overexpressing HIF-1α promotes angiogenesis and muscular tissue repair in a hind limb ischemia model, *J. Controlled Release*, 2020, **322**, 610–621.
32 L. Saludas, E. Garbayo, A. Ruiz-Villalba, S. Hernández, P. Vader, F. Prósper and M. J. Blanco-Prieto, Isolation methods of large and small extracellular vesicles derived from cardiovascular progenitors: A comparative study, *Eur. J. Pharm. Biopharm.*, 2022, **170**, 187–196.
33 H. Niiyama, N. F. Huang, M. D. Rollins and J. P. Cooke, Murine Model of Hindlimb Ischemia, *J. Visualized Exp.*, 2009, 1035.
34 E. Stabile, M. S. Burnett, C. Watkins, T. Kinnaird, A. Bachis, A. la Sala, J. M. Miller, M. Shou, S. E. Epstein and S. Fuchs, Impaired arteriogenic response to acute hindlimb ischemia in CD4-knockout mice, *Circulation*, 2003, **108**, 205–210.
35 W. Du, K. Zhang, S. Zhang, R. Wang, Y. Nie, H. Tao, Z. Han, L. Liang, D. Wang, J. Liu, N. Liu, Z. Han, D. Kong, Q. Zhao and Z. Li, Enhanced proangiogenic potential of mesenchymal stem cell-derived exosomes stimulated by a nitric oxide releasing polymer, *Biomaterials*, 2017, **133**, 70–81.
36 I. S. Park, C. Mahapatra, J. S. Park, K. Dashnyam, J. W. Kim, J. C. Ahn, P. S. Chung, D. S. Yoon, N. Mandakhbayar, R. K. Singh, J. H. Lee, K. W. Leong and H. W. Kim, Revascularization and limb salvage following critical limb ischemia by nanoceria-induced Ref-1/APE1-dependent angiogenesis, *Biomaterials*, 2020, **242**, 119919.
37 L. C. Duke, A. S. Cone, L. Sun, D. P. Dittmer, D. G. Jr. Meckes and R. J. Tomko Jr, Tetraspanin CD9 alters cellular trafficking and endocytosis of tetraspanin CD63, affecting CD63 packaging into small extracellular vesicles, *J. Biol. Chem.*, 2025, **301**, 108255.
38 T. Seibold, M. Waldenmaier, T. Seufferlein and T. Eiseler, Small Extracellular Vesicles and Metastasis-Blame the Messenger, *Cancers*, 2021, **13**, 4380.
39 J. Han, L. Luo, O. Marcelina, V. Kasim and S. Wu, Therapeutic angiogenesis-based strategy for peripheral artery disease, *Theranostics*, 2022, **12**, 5015–5033.
40 H. Zhou, T. Chen, Y. Li, J. You, X. Deng, N. Chen, T. Li, Y. Zheng, R. Li, M. Luo, J. Wu and L. Wang, Glycation of Tie-2 Inhibits Angiopoietin-1 Signaling Activation and

Angiopoietin-1-Induced Angiogenesis, *Int. J. Mol. Sci.*, 2022, **23**, 7137.

41 Y. Zhao, B. Yu, Y. Wang, S. Tan, Q. Xu, Z. Wang, K. Zhou, H. Liu, Z. Ren and Z. Jiang, Ang-1 and VEGF: central regulators of angiogenesis, *Mol. Cell. Biochem.*, 2025, **480**, 621–637.

42 W. T. Meng and H. D. Guo, Small Extracellular Vesicles Derived from Induced Pluripotent Stem Cells in the Treatment of Myocardial Injury, *Int. J. Mol. Sci.*, 2023, **24**, 4577.

43 C. Cavallari, A. Ranghino, M. Tapparo, M. Cedrino, F. Figliolini, C. Grange, V. Giannachi, P. Garneri, M. C. Deregibus, F. Collino, P. Rispoli, G. Camussi and M. F. Brizzi, Serum-derived extracellular vesicles (EVs) impact on vascular remodeling and prevent muscle damage in acute hind limb ischemia, *Sci. Rep.*, 2017, **7**, 8180.

44 Z. Erana-Perez, M. Igartua, E. Santos-Vizcaino and R. M. Hernandez, Differential protein and mRNA cargo loading into engineered large and small extracellular vesicles reveals differences in in vitro and in vivo assays, *J. Controlled Release*, 2025, **379**, 951–966.

45 H.-D. Cho, J.-H. Kim, J.-K. Park, S.-M. Hong, D.-H. Kim and K.-I. Seo, Kochia scoparia seed extract suppresses VEGF-induced angiogenesis via modulating VEGF receptor 2 and PI3K/AKT/mTOR pathways, *Pharm. Biol.*, 2019, **57**, 684–693.

46 Z. Zhang, L. Niu, X. Tang, R. Feng, G. Yao, W. Chen, W. Li, X. Feng, H. Chen and L. Sun, Mesenchymal stem cells prevent podocyte injury in lupus-prone B6.MRL-Faslpr mice via polarizing macrophage into an anti-inflammatory phenotype, *Nephrol., Dial., Transplant.*, 2019, **34**, 597–605.

47 L. Liao, Y. Tang, Y. Zhou, X. Meng, B. Li and X. Zhang, MicroRNA 126 (MiR 126): key roles in related diseases, *J. Stress Physiol. Biochem.*, 2024, **80**, 277–286.

48 S. Kholia, A. Ranghino, P. Garnieri, T. Lopatina, M. C. Deregibus, P. Rispoli, M. F. Brizzi and G. Camussi, Extracellular vesicles as new players in angiogenesis, *Vasc. Pharmacol.*, 2016, **86**, 64–70.

49 A. A. Salybekov, A. Salybekova, Y. Sheng, Y. Shinozaki, K. Yokoyam, S. Kobayashi and T. Asahara, Extracellular Vesicles Derived From Regeneration Associated Cells Preserve Heart Function After Ischemia-Induced Injury, *Front. Cardiovasc. Med.*, 2021, **8**, 754254.

50 W.-T. Chen, Y. Luo, X.-M. Chen and J.-H. Xiao, Role of exosome-derived miRNAs in diabetic wound angiogenesis, *Mol. Cell. Biochem.*, 2024, **479**, 2565–2580.